

# The *Petunia* Ortholog of *Arabidopsis* *SUPERMAN* Plays a Distinct Role in Floral Organ Morphogenesis

Hitoshi Nakagawa,<sup>a</sup> Silvia Ferrario,<sup>b</sup> Gerco C. Angenent,<sup>b</sup> Akira Kobayashi,<sup>a,1</sup> and Hiroshi Takatsujii<sup>a,2</sup>

<sup>a</sup>Developmental Biology Laboratory, Plant Physiology Department, National Institute of Agrobiological Sciences, Tsukuba, Ibaraki 305-8602, Japan

<sup>b</sup>Business Unit Plant BioScience, Plant Research International, 6700 AA Wageningen, The Netherlands

*Arabidopsis* (*Arabidopsis thaliana*) *SUPERMAN* (*SUP*) plays a role in establishing a boundary between whorls 3 and 4 of flowers and in ovule development. We characterized a *Petunia hybrida* (*petunia*) homolog of *SUP*, designated *PhSUP1*, to compare with *SUP*. Genomic DNA of the *PhSUP1* partially restored the stamen number and ovule development phenotypes of the *Arabidopsis sup* mutant. Two *P. hybrida* lines of transposon (*dTph1*) insertion mutants of *PhSUP1* exhibited increased stamen number at the cost of normal carpel development, and ovule development was defective owing to aberrant growth of the integument. Unlike *Arabidopsis sup* mutants, *phsup1* mutants also showed extra tissues connecting stamens, a petal tube and an ovary, and aberrancies in the development of anther and placenta. *PhSUP1* transcripts occurred in the basal region of wild-type flowers around developing organ primordia in whorls 2 and 3 as well as in the funiculus of the ovule, concave regions of the placenta, and interthecal regions of developing anthers. Overexpression of *PhSUP1* in *P. hybrida* resulted in size reduction of petals, leaves, and inflorescence stems. The shortening of inflorescence stems and petal tubes was primarily attributable to suppression of cell elongation, whereas a decrease in cell number was mainly responsible for the size reduction of petal limbs.

## INTRODUCTION

Flowers of many angiosperms are composed of four kinds of organ that arise in four concentric whorls: sepal in the outermost whorl (whorl 1), petal in whorl 2, stamen in whorl 3, and carpel in the innermost whorl (whorl 4) (Smyth et al., 1990). The number of floral organs in each whorl and the arrangement of the organs within the whorl are genetically determined. The patterning of floral whorls has been explained by the ABC model; the identity of floral organs that generate in each whorl is specified by combinatorial interaction of three classes of homeotic genes, A, B, and C, each of which is expressed in two adjacent whorls (Yanofsky et al., 1990; Jack et al., 1992; Goto and Meyerowitz, 1994). The floral homeotic genes, which mostly encode MADS box-type transcription factors, are conserved among angiosperms. Several studies have demonstrated that the ABC model fundamentally applies to many plant species that have various structures and reproductive systems of flowers. By contrast, the mechanisms for determining the number and position of floral organs in each whorl have been much less studied. The size of floral meristem in respective whorls is a key determinant of the

number of floral organs. For instance, *Arabidopsis* (*Arabidopsis thaliana*) *clavata* mutants have enlarged floral meristems, and the total number of their floral organs is increased in proportion to the size of the meristem (Clark et al., 1993). Similarly, the organ number in each whorl seems to be correlated with the size of the whorl (Meyerowitz, 1997), but less is understood about how the number of each type of floral organ is determined.

*Arabidopsis superman* (*sup*) mutants have an increased number of stamens and defective pistil (Schultz et al., 1991; Bowman et al., 1992). The *SUP* gene is expressed in the subdomain of whorl 3 adjacent to whorl 4 during a very early stage of flower development (Sakai et al., 1995). This expression is dependent on the floral meristem gene *LEAFY* and two class B homeotic genes, *APETALLA3* (*AP3*) and *PISTILLATA* (*PI*) (Sakai et al., 2000). On the basis of expression and epistasis studies, as well as the phenotype attributable to constitutive expression of *AP3* and *PI* in the *sup* background (Krizek and Meyerowitz, 1996), *SUP* is thought to coordinate proliferation of stamen- and carpel-specific meristematic cells, keeping the proper structure of whorls and maintaining the boundary between whorl 3 and whorl 4 at the right position (Sakai et al., 2000). Ectopic expression of *SUP* in *Nicotiana tabacum* (tobacco) plants causes a decrease in cell number in various organs, resulting in reduction in the sizes of those organs (Bereterbide et al., 2001). This observation supports the involvement of *SUP* in the control of cell proliferation. Another report proposes a role of *SUP* in cell elongation on the basis of the phenotype resulting from ectopic expression of *SUP* in petals and stamens of *Petunia hybrida* (*petunia*) (Kater et al., 2000). In addition to the early floral meristem function we have just described, *SUP* plays a role in the development of ovules (Gaiser et al., 1995). Normal ovules have a hood-like morphology because of asymmetric growth of the outer integument. By

<sup>1</sup> Current address: Department of Upland Agriculture Research, National Agriculture Research Center for Hokkaido Region, Shinsei, Memuro, Hokkaido 082-0071, Japan.

<sup>2</sup> To whom correspondence should be addressed. E-mail takatsuh@nias.affrc.go.jp; fax 81-29-838-8383.

The author responsible for distribution of materials integral to the findings presented in this article in accordance with the policy described in the Instructions for Authors (www.plantcell.org) is: Hiroshi Takatsujii (takatsuh@nias.affrc.go.jp).

Article, publication date, and citation information can be found at www.plantcell.org/cgi/doi/10.1105/tpc.018838.



protein. The EAR-like motif in SUP has been demonstrated to act as an active transcriptional repressor domain (Hiratsu et al., 2002). Sequence comparison between *PhSUP1* cDNA and the corresponding genomic sequence revealed that the *PhSUP1* gene lacks introns.

### *PhSUP1* Partially Complements the Arabidopsis *sup* Mutant

To test whether *PhSUP1* is functionally equivalent to Arabidopsis *SUP*, we introduced a 3.8-kb genomic DNA fragment containing the 5'-upstream (2.5 kb), coding, and 3'-untranslated (UTR) (0.46 kb) regions of *PhSUP1* (*gPhSUP1*) into an Arabidopsis *sup* mutant. In wild-type *Arabidopsis*, a flower consists of four sepals, four petals, six stamens, and one pistil (Figure 2A). The ovules are hood-like owing to asymmetric growth of the outer integument (Figure 2G) (Gaiser et al., 1995). Almost all wild-type *Arabidopsis* flowers were fertile (i.e., 323 out of 324 flowers set seeds after flowering). By contrast, flowers of the *sup* mutant (*sup2*) had an increased number of stamens ( $8.6 \pm 1.6$ ;  $n = 45$ , from three plants) at the expense of normal pistil development (Figure 2B).

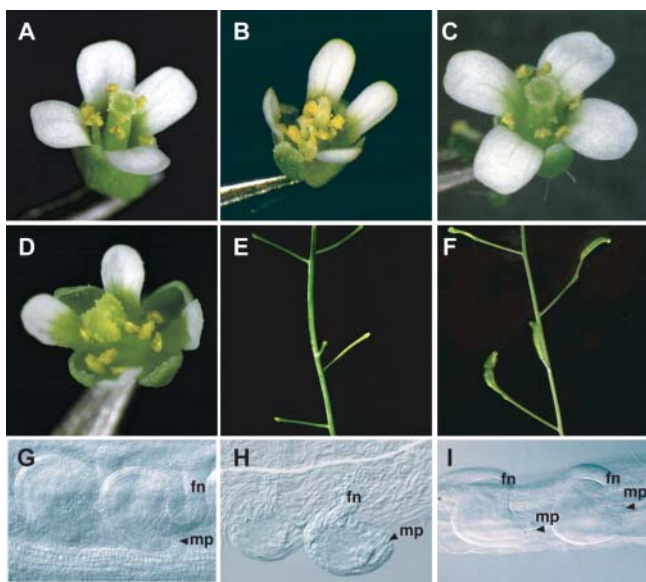


**Figure 2.** Complementation of Arabidopsis *sup* Mutants by *PhSUP1* Genomic DNA.

(A) to (D) Flowers of wild-type (A) and *sup* mutant (B) *Arabidopsis* plants and those of a *sup(PhSUP1)* plant that contains a *PhSUP1* genomic fragment as a transgene (C) and (D)]. Flowers in the *sup(PhSUP1)* plants showed almost complete (C) or weak (D) recovery of flower development.

(E) and (F) Inflorescence in *sup* mutant (E) and *sup(PhSUP1)* plants (F) after flowering. The *sup* mutant produced no fertilized siliques (E), whereas *sup(PhSUP1)* plants frequently produced them (F).

(G) to (I) Ovules in wild-type (G), *sup* mutant (H), and *sup(PhSUP1)* (I) plants. Siliques in the *sup(PhSUP1)* plant contained both *sup*-like (left) and wild-type-like (right) ovules. The top of the pistil is at the right. fn, funiculus; mp, micropyle.

Ovules in the *sup* mutant lacked asymmetry in the growth of the outer integument (Figure 2H) (Gaiser et al., 1995). Because of these aberrancies in the development of the pistil and ovules, the *sup* mutant had severely reduced fertility (i.e., only 8 of 342 flowers from three plants set seeds) (Figure 2E).

Introduction of the *gPhSUP1* sequence markedly recovered the developmental aberrancies in *sup* mutants (Figures 2C and 2D). Compared with the *sup* mutant, the *gPhSUP1*-transformed *sup* mutants (*gPhSUP1/sup*) had fewer stamens ( $6.9 \pm 0.9$ ,  $n = 45$ , from three plants) and partially restored normal pistil morphology (Figure 2C). Whereas normal pistils are rarely formed in *sup* mutants, 27% of the flowers of *gPhSUP1/sup* plants had normal-looking pistils (Figure 2C). Stamen–pistil mosaic organs formed in many *gPhSUP1/sup* flowers (Figure 2D), but their staminoid feature was less prominent than that in the *sup* mutant. Most *gPhSUP1/sup* flowers contained ovules in their ovaries, whereas half of the *sup* flowers completely lacked ovules. In the ovaries of the *gPhSUP1/sup* plants, both normal-looking and *sup*-like ovules were present (Figure 2I), and the proportion of normal-looking ovules increased toward the apical tip of the pistil. Because of the partial restoration to a normal morphology of their pistils and ovules, the *gPhSUP1/sup* plants partially recovered female fertility (i.e., 58 of 343 flowers from three plants were fertile) (Figure 2F). These results indicate that *PhSUP1* is an ortholog of *SUP*.

### *PhSUP1* Knockout Mutants Have a *sup*-Like Phenotype

To characterize the loss-of-function phenotype of *PhSUP1*, we screened a library of transposon (*dTph1*)-inserted mutant lines of *P. hybrida* (Koes et al., 1995) and obtained two recessive insertional alleles for *PhSUP1* (*phsup1-tm1* and *phsup1-tm2*, Figure 1A). The *phsup1-tm1* allele had a *dTph1* insertion immediately upstream of the zinc-finger domain, causing interruption of the reading frame. Because the *phsup1-tm1* allele encodes only a short truncated protein that lacks both the zinc-finger and Leu zipper/EAR motif-like sequences, it is most likely a nonfunctional allele. The other allele, *phsup1-tm2*, contained a *dTph1* insertion upstream of the Leu zipper/EAR-like motif, resulting in the replacement of the C-terminal 37 residues, including the putative repressor domain with an unrelated sequence. Because both mutant alleles had the same phenotype, the *phsup1-tm2* also was presumed to be a null allele. RNA gel blot analysis detected low levels of *PhSUP1*-derived transcripts of slightly increased sizes because of the *dTph1* insertion in both alleles (Figure 1B). The phenotypes observed in these mutants were multifaceted: some of them mimicked those in Arabidopsis *sup* mutants, but others were unique to the *phsup1* mutants.

The nongenerative organs of the *phsup1* mutants were apparently normal. Floral organs of the outer three whorls (sepals, petals, and stamens) were also indistinguishable from those of wild-type *P. hybrida*; however, whorl 4 organs showed remarkable aberrancies in their number and characteristics. Whorl 4 of wild-type *P. hybrida* flowers forms a pistil that generates by fusion of two carpels and consists of a stigma, a long style, and a small conical ovary (Figures 3D and 3J). In whorl 4 of *phsup1* flowers, one to three extra stamens were formed, and the pistils

often comprised one, three, or four carpels (Figures 3B, 3C, 3E, and 3K to 3M). The extra stamens were frequently fused with the pistil to various extents (Figures 3L and 3M). For instance, the flower in Figure 3L has two extra stamens, with one of them fused to the ovary at its base and the other fused to the pistil almost throughout the organ. In a severe case, two extra stamens were completely fused to a pistil, and they developed as antheroid sectors in a stamen–carpel mosaic organ (Figure 3M). In such a chimeric organ, a whitish stripe of stamen filament–like tissue can be distinguished below the antheroid tissue (Figure 3M). Carpels were usually incompletely fused with each other, and each was tipped by a stigma (Figures 3B, 3C, and 3M). Some mutant flowers did not contain extra stamens; instead, they

contained a pistil consisting of three carpels (Figure 3K). In this case as well, the style showed a stamen filament–like feature. These phenotypes are similar to those in *Arabidopsis sup* mutants (Schultz et al., 1991; Bowman et al., 1992), further indicating that *PhSUP1* is a *P. hybrida* counterpart of *SUP*.

The wild-type ovary is conical and is located at the base of a flower (Figures 3A and 3J). The ovules are formed throughout the placenta (Figure 3N). By contrast, in the *phsup1* mutants, the ovary is thin and elongated (Figures 3B, 3C, and 3K to 3M), and far fewer ovules were formed than in wild-type ovaries (Figure 3O). The aberrancies observed in the morphology of *phsup1* ovules are similar to those reported for the *Arabidopsis sup* ovules (Gaiser et al., 1995). Unlike *Arabidopsis* ovules, which

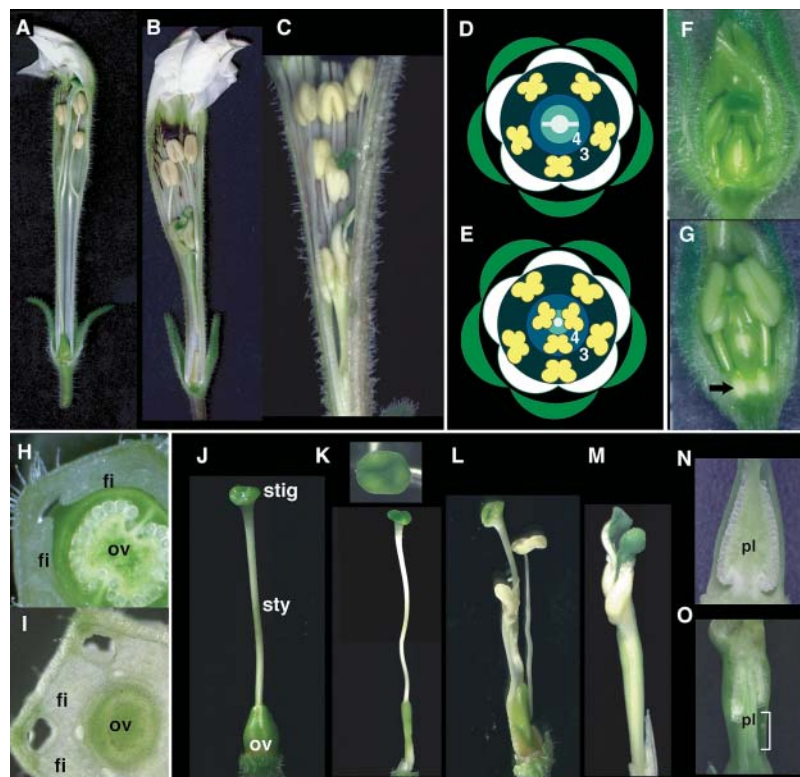


**Figure 3.** Phenotypes of *phsup1* Mutants in Flower Development.

The wild-type flower consists of four concentric whorls of organs: five sepals, five petals, five stamens, and a pistil composed of two carpels. Whorl 3 (3) and whorl 4 (4) organs are indicated. Number and identity of organs in whorls 1, 2, and 3 in *phsup1* mutant flowers are the same as those in the wild type, but two or three extra stamens were generated in whorl 4.

(A) to (C) Side views of *P. hybrida* flowers in wild-type (A) and *phsup1-tm1* ([B] and [C]) plants. A few petals and sepals have been removed to show whorl 4 organs.

(D) and (E) Flower diagrams of wild-type (D) and *phsup1* mutant (E) flowers.

(F) and (G) Side views of 10-mm flower buds in wild-type (F) and *phsup1-tm1* (G) plants. Extra tissues are seen at the bases of whorl 3 stamens in *phsup1-tm1* flowers as indicated by an arrow (G).

(H) and (I) Transverse sections at the basal part of 10-mm flower buds in wild-type (H) and *phsup1-tm1* (I) plants. fi, filament; ov, ovary.

(J) to (M) Whorl 4 organs in wild-type (J) and *phsup1-tm1* ([K] to [M]) plants. Wild-type pistils consist of two fused carpels (J). In *phsup1-tm1*, pistils often consisted of three carpels, and the style shows a stamen filament–like feature (K). Extra stamens were frequently generated and were usually fused with a pistil to various extents ([L] and [M]) (i.e., stamens were fused with an ovary at the base of their filaments [L] or fused with a style throughout the entire filament [M]). ov, ovary; stig, stigma; sty, style.

(N) and (O) Ovaries in wild-type (N) and *phsup1-tm1* (O) plants. The bottom of the placenta was elongated in *phsup1-tm1* ovaries as indicated. pl, placenta.



have two layers (inner and outer) of integument, *P. hybrida* has only a single layer of integument. The wild-type ovule has a bilaterally symmetrical hood-like morphology, and the micropyle is adjacent to the funiculus (Figures 4A and 4B) because the integument grows exclusively at the adaxial side (toward the top of the ovary). By contrast, the integument of *phsup1* mutants grew evenly around a nucellus, forming nearly radially symmetrical tubular ovules (Figures 4C and 4D); consequently, the micropyle is positioned at the top of the ovule (Figure 4D).

### *PhSUP1* Plays a Role in the Morphogenesis of Various Floral Organs

In addition to the phenotypes that are like those of *Arabidopsis sup* mutants, *phsup1* mutants also displayed additional aberrancies in the morphologies of various floral organs. In wild-type *P. hybrida* flowers, the stamen filaments are flat at their basal parts and are tightly fused with the petal tube (Figure 3H). In the *phsup1* flower, unusual tissues consisting of highly vacuolated cells were generated around the filaments (Figures 3G and 3I). Presumably, these extra tissues resulted from excessive proliferation of the cells that normally form junctions between stamen filaments and petal tubes.

The *phsup1* mutants were also defective in the shape of anthers (Figures 5A to 5D). The mature anther normally consists of two distinctively partitioned thecae with an intertheal furrow between them, and each theca consists of two locules (Figure 5E). In mature anthers in *phsup1* mutants, the two thecae appear to be fused in the upper part at the adaxial side of the anther (Figure 5G, c). The lower part is apparently normal, but

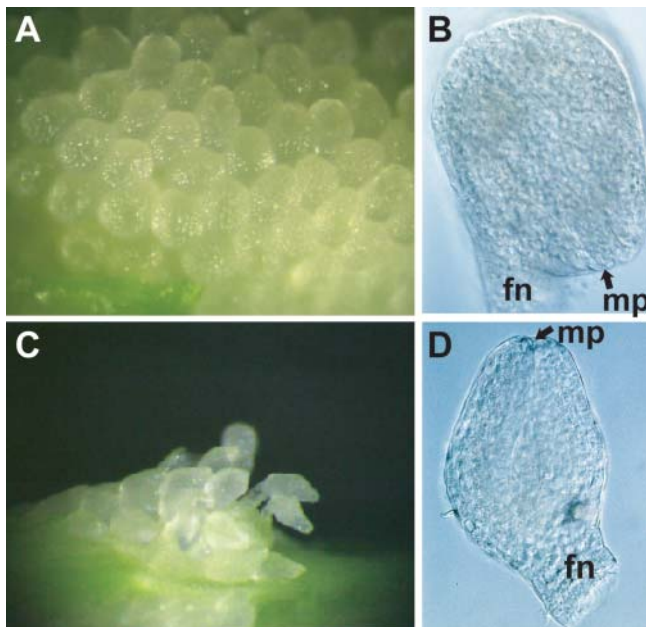


**Figure 4.** *phsup1* Mutant Phenotypes in Ovules.

Stereomicroscopic images of ovules in wild-type (A) and *phsup1-tm1* (C) and differential interference contrast optics of a cleared ovule in wild-type (B) and *phsup1-tm1* (D). fn, funiculus; mp, micropyle.

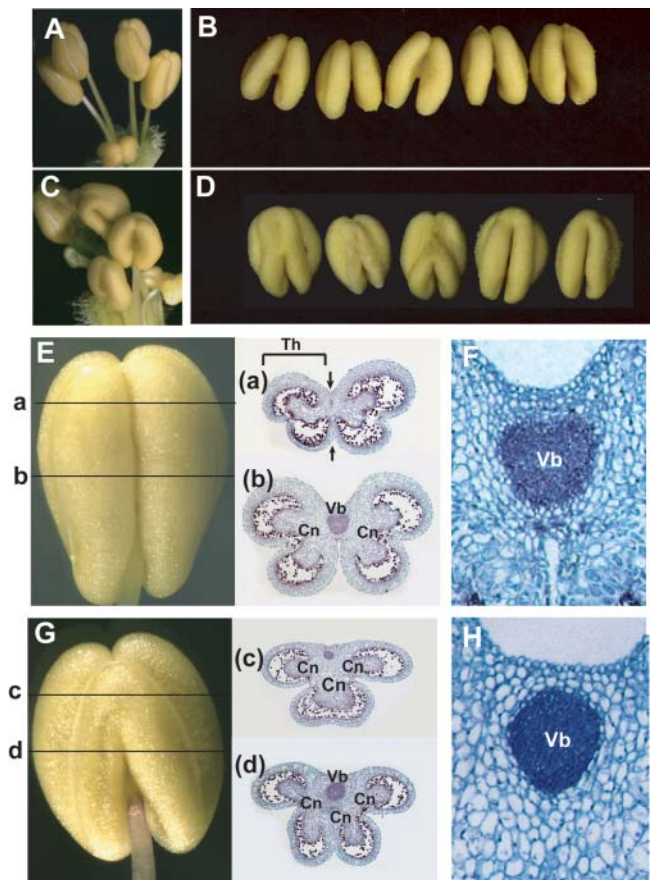


**Figure 5.** *phsup1* Mutant Phenotype in Anthers.

(A) to (D) Anthers in wild-type (A) and (B) and *phsup1-tm1* (C) and (D) plants.

(E) and (G) A mature wild-type anther and its transverse sections at positions a and b (E) and a mature *phsup1-tm1* anther and its transverse sections at positions c and d (G). Cn, connective tissue; Th, theca; Vb, vascular bundle.

(F) and (H) Close-up views of the transverse sections at lower parts of developing anthers around a vascular bundle in the wild-type (F) and *phsup1-tm1* (H) anthers. Arrows in E-a indicate intertheal furrows. Vb, vascular bundle.

its transverse section revealed an abnormal development around the vascular bundle (Figures 5G, d and 5H). In wild-type anthers, intertheal furrows are well developed, which makes the anther walls closely bound to the vascular bundle (Figures 5E, a; 5E, b; and 5F). By contrast, the anther walls of *phsup1* mutants were less closely bound to the vascular bundle, with excessively proliferated connective tissue intervening (Figures 5G, c; 5G, d; and 5H). Close-ups of the vascular bundles of wild-type anthers revealed that cells at the intertheal furrow at both the adaxial and abaxial sides of the vascular bundle are smaller than the cells in neighboring regions (Figure 5F). By contrast, the cells in the corresponding regions of *phsup1* mutant anthers are the same size as those in neighboring regions (Figure 5H).

### Scanning Electron Microscopy Analysis at Early-Stage Flower Development

Using scanning electron microscopy, we investigated the early-stage development of stamens in wild-type and *phsup1* mutant flowers. There was no difference in size and dome-shaped morphology of stamen primordia between wild-type (Figures 6A and 6B) and *phsup1* mutant (Figures 6E and 6F) flowers at early stages. Later, longitudinal hollows formed at the adaxial side of wild-type anthers (Figure 6C), and they subsequently developed into interthecal furrows (Figure 6D). The wild-type anther then separated into four locules (Figures 6I). In *phsup1* mutant flowers at these stages, aberrancies in the development of interthecal furrows were observed; in particular, the top parts at the adaxial side of developing anthers failed to separate into two inner locules (Figures 6H and 6J to 6L).

In wild-type *P. hybrida*, two carpel primordia are initiated as horseshoe-shaped banks within whorl 4 when stamen primordia become dome-shaped (Figure 6B). These two carpel primordia are fused at the base (Figure 6C) and grow vertically as a slotted tube (Figure 6D). Subsequently, the bicarpellate pistil becomes fused at the top to form the style and stigma, completing the

ontogeny of a wild-type pistil (Figure 6I). In the *phsup1* mutant flower, initiation of whorl 4 organs was delayed (Figures 6F and 6G). Later, two to four organ primordia were initiated within a ring interior to whorl 3 (Figure 6H), and these organ primordia started to differentiate into extra stamens, carpels, or stamen–carpel mosaic organs (Figures 6J to 6L). The one or two primordia that initiated early tended to develop as extra stamens, and the other late-initiating ones develop as pistils or stamen–carpel mosaic organs (Figures 6J and 6K). In some cases, three organ primordia developed as carpels (Figure 6L) and fused to form a tricarpellate pistil (Figure 3K).

### Expression of *PhSUP1*

Distribution of *PhSUP1* transcripts in developing flower organs was examined by in situ hybridization. At stages when organ primordia begin to differentiate, *PhSUP1* transcripts were detected at the basal region of developing whorl 2 and whorl 3 organs (Figure 7A). Transverse sections showed that the expression was distributed in marginal regions between organ primordia and was excluded from the organ primordia themselves

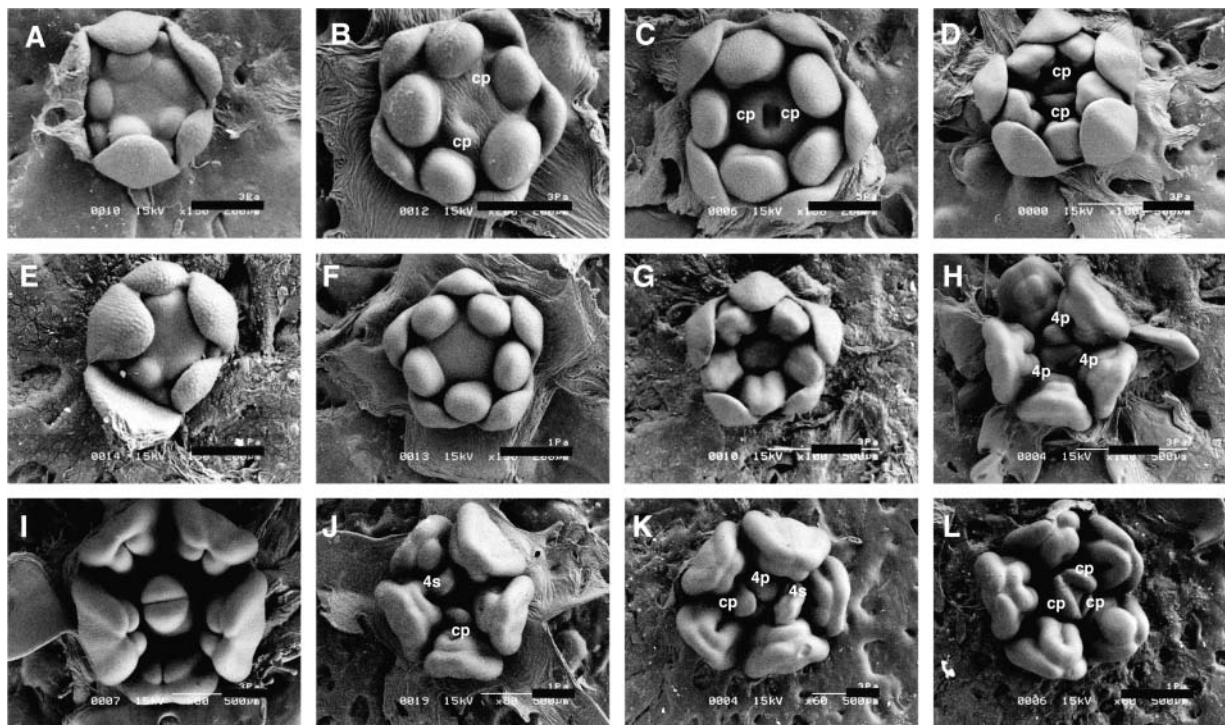


**Figure 6.** Scanning Electron Micrographs Depicting Flower Development.

(A) to (D) and (I) Development of wild-type flowers. In each stage, petal and sepal primordia arise (A), stamen primordia become dome-shaped and carpel primordia arise (B), stamen primordia are stalked and carpels are fused at the base (C), and then the carpel grows vertically as a slotted tube (D). Later, anther locules are formed, the gynoecium fuses at the top, and stigma and style appear (I). cp, carpel primordia.

(E) to (H) and (J) to (L) Development of *phsup1-tm1* mutant flowers. Stages of *phsup1-tm1* mutant flower in (E), (F), (G), and (H) correspond to those of wild-type flowers in (A), (B), (C), and (D), respectively. No sign of whorl 4 organ initiation is seen in early stages ((E) to (G)). In a following stage, a ring of three organ primordia (4p) initiates interior to whorl 3 stamens (H), and various patterns of organs appear in whorl 4. Outer whorls of flowers have been removed to show inner organs. 4p, undifferentiated whorl 4 organ primordia; 4s, whorl 4 stamen primordia; cp, carpel primordia.

Bar = 200  $\mu$ m.

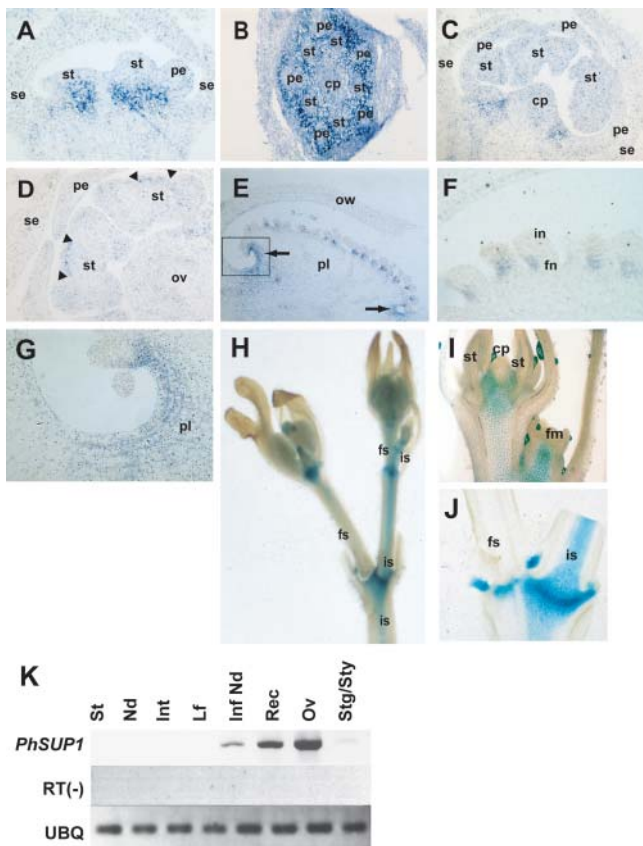


**Figure 7.** Expression Pattern of *PhSUP1* Gene.

(A) to (D) In situ hybridization of *PhSUP1* transcripts in developing flower. Longitudinal (A) and (C) and transverse (B) sections of flower buds are shown. The stage of flower in (A) and (B) corresponds to that in Figure 6B, (C) corresponds to Figure 6C, and (D) corresponds to Figure 6I. In (D), bands of expression are indicated by pairs of closed triangles. cp, carpel; ov, ovary; pe, petal; se, sepal; st, stamen.

(E) to (G) In situ hybridization of *PhSUP1* transcripts in a young ovary. Shown are a longitudinal section of an ovary (E), a higher-magnification view of ovules (F), and a close-up of basal part of placenta (G), boxed area in (E). In (E), top and bottom of the ovary are shown to the right and left in the panel, respectively, and *PhSUP1* transcripts in the placenta are indicated by arrows. ow, ovary wall; pl, placenta; in, integument; fn, funiculus.

(H) to (J) Histochemical staining of GUS activity driven by *PhSUP1* promoter in the inflorescence (H), a young flower bud (I), and an inflorescence node (J). st, stamen; cp, carpel; fm, floral meristem; fs, flower stalk; is, inflorescence stalk.

(K) RT-PCR analysis of *PhSUP1* transcripts in vegetative and floral organs from 10-mm flower buds. St, shoot tip; Nd, vegetative stem node; Int, stem internode; Lf, leaf; Inf Nd, inflorescence node; Rec, receptacle; Ov, ovary; Stg/Sty, stigma/style; UBQ, ubiquitin.

(Figures 7B). *PhSUP1* transcripts also were detected in developing anthers as bands of signals in the interthecal region after the formation of thecae (Figure 7D). At later stages, *PhSUP1* expression appeared in the funiculi that constitute the basal part of the ovule (Figures 7E and 7F). Distribution of *PhSUP1* tran-

scripts in the funiculi was asymmetric: they were localized at the side abaxial to that in which the growth of the integument is suppressed. *PhSUP1* also was expressed at the top and bottom parts of the developing placenta, where the organ is concave and free of ovules (Figures 7E and 7G). The concave area at the bottom of the placenta remains in the mature flower, whereas that at the top of placenta has disappeared because of the outgrowth of style (Figure 3N). In the mature flower of *phsup1* mutants, the concave area at the bottom of placenta is lost; instead, the corresponding regions are elongated (Figure 3O), suggesting a role of *PhSUP1* in the morphogenesis of the placenta.

To investigate the expression of *PhSUP1* in other parts of plants, we constructed transgenic *P. hybrida* plants harboring a recombinant reporter gene that is comprised of a 2.5-kb 5'-upstream region of *PhSUP1* fused upstream of the  $\beta$ -glucuronidase (*GUS*) coding sequence (*PhSUP1*:*GUS*). Three independent *PhSUP1*:*GUS* transgenic plants were characterized for promoter activity. In young flowers, the *PhSUP1*:*GUS* plants expressed *GUS* activity in the ovary and at boundary regions between developing stamens and carpels (Figure 7I), consistent with the results of in situ hybridization experiments (Figure 7C). In addition, the expression extended into receptacles and piths in inflorescent stems. A recent study by Ito et al. (2003) demonstrated that negative *cis* elements determining whorl-specific expression of *SUP* are located in the coding region. Because our *PhSUP1*:*GUS* construct does not include the coding region, it is quite possible that the lack of certain negative elements resulted in the ectopic promoter activity. The upstream region of *SUP* between  $-3$  and  $-5$  kb contains *cis* elements for early expression (Ito et al., 2003). Our *PhSUP1*:*GUS* construct contains only up to  $-2.5$  kb of upstream sequence, which could also affect the accuracy of the promoter activity. Figures 7H and 7J show *GUS* activity in the inflorescence, with particularly strong activity at the nodal region. The *GUS* activity in the inflorescence is stronger in inflorescence stalks than in flower stalks (Figures 7H and 7J). In an RT-PCR experiment, *PhSUP1* transcripts were detected in the inflorescence nodes (among vegetative tissues) and in the ovary and receptacle but not in stigmas or styles of developing flowers, consistent with the results of the promoter-*GUS* experiments (Figure 7K). These results suggest that *PhSUP1* plays a role in the growth of inflorescences as well. However, we did not find any visible aberrancy in the growth of inflorescence in the *phsup1* mutants.

### Phenotype of Plants Overexpressing *PhSUP1*

To characterize the effects of ectopic expression of *PhSUP1*, its cDNA was driven by the 35S promoter of *Cauliflower mosaic virus* (CaMV) in transgenic *P. hybrida* plants. Two lines were found to overexpress *PhSUP1*, and they both showed the same dwarf phenotype (*PhSUP1*-ox plants, Figure 8A). The overexpression of *PhSUP1* caused reduction in the sizes of flower organs by an average of 60 to 70% compared with wild-type organs, with the most severe reduction being in the petal limbs ( $\sim 30\%$  of wild type, Figure 8B). The leaves were also smaller than those of wild-type plants and were curled up at their margins (Figure 8C). The inflorescence of *P. hybrida* consists of two types



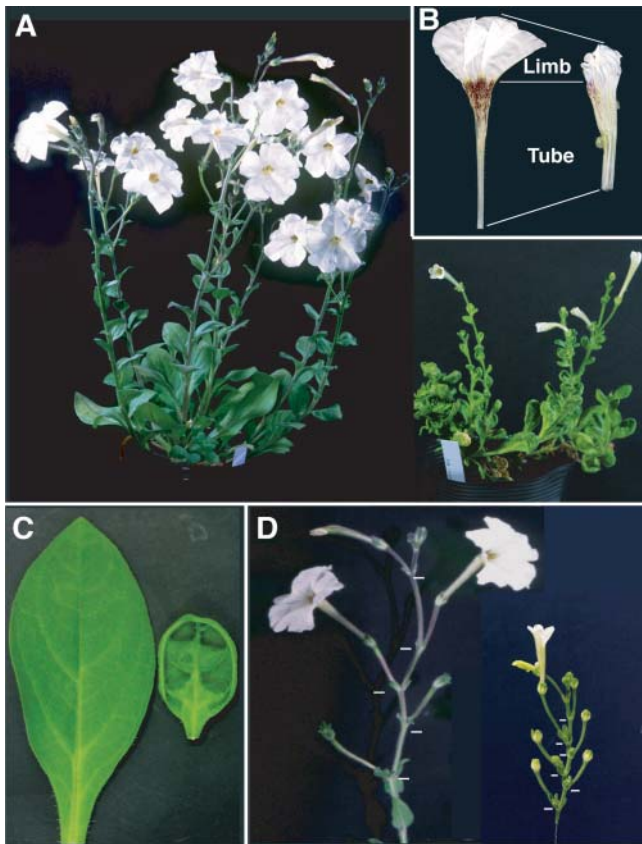


**Figure 8.** Phenotype of a *PhSUP1*-Overexpressing *P. hybrida*.

Wild-type and *PhSUP1*-ox phenotypes are shown at the left and right in the panels, respectively. Bars in **(D)** indicate positions of inflorescence nodes.

- (A)** Whole plants.  
**(B)** Flowers.  
**(C)** Leaves.  
**(D)** Inflorescences.

of stem: the pedicel (floral stalk) terminates in a flower, and the peduncle (inflorescence stalk) constitutes a main stem. The internodes of the peduncles in *PhSUP1*-ox plants were shortened by  $\sim 30\%$  compared with those in wild-type plants, whereas pedicels were only slightly shortened ( $\sim 85\%$  of wild type, Figure 8D).

Scanning electron microscopy revealed that *PhSUP1* overexpression markedly suppressed the longitudinal growth of the epidermal cells in the peduncles (Figures 9A and 9B). The length of the epidermal cells in the peduncle was  $\sim 40\%$  of the wild type, a difference that is nearly proportional to the suppression in the length of peduncle (Table 1). The size of the pedicel epidermal cells was 82% of the wild type (Table 1), which is also proportional to the suppression in the pedicel length. Longitudinal sections of a peduncle revealed that the elongation of inner cells also was affected in a similar manner to that in the epidermal cells (Figures 9C and 9D). These results indicate that suppression of

inflorescence growth in *PhSUP1*-ox plants is primarily attributable to suppression of cell elongation.

Scanning electron microscopy of the adaxial surface of petals revealed that the sizes of epidermal cells in the petal limb of *PhSUP1*-ox plants were comparable with those in wild-type plants (Table 1). These observations indicate that the shortening of the petal limb is mainly because of a decrease in cell number. By contrast, the reduction in the length of the petal tube was nearly proportional to the reduction in the length of cells (78% of the wild type), suggesting that suppression of cell elongation is the main cause for the reduced growth of petal tubes (Figure 8B).

*PhSUP1* overexpression also affected the morphology and sizes of cells in leaf mesophyll tissues (Figures 9E and 9F). Wild-type leaf mesophyll tissue is distinctively differentiated into two types of cell layer: two to three layers of palisade cells at the adaxial side and four to five layers of spongy cells with increased intercellular space along the abaxial side (Figure 9E). By contrast, the leaf mesophyll tissue in the *PhSUP1*-ox plant was not clearly differentiated into the two cell types, instead appearing as a homogeneous tissue consisting of only spongy cells (Figure 9F). The number of mesophyll cell layers and total number of cells were clearly decreased, whereas individual cells are expanded.

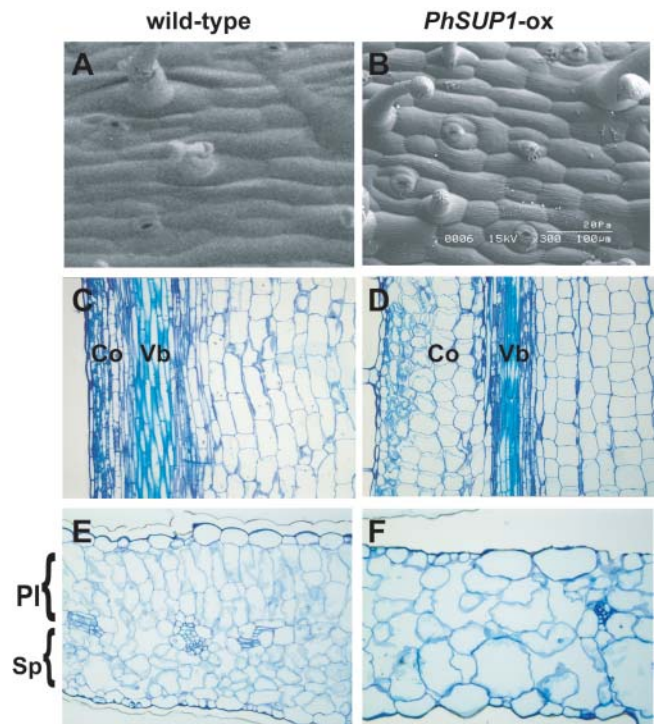


**Figure 9.** Effects of *PhSUP1* Overexpression on Cellular Morphology.

**(A)** and **(B)** Scanning electron microscopy images of peduncle epidermal cells in wild-type **(A)** and *PhSUP1*-ox **(B)** *P. hybrida* plants. The shoot apex is oriented to the left in the panels.

**(C)** and **(D)** Longitudinal sections of peduncles in wild-type **(C)** and *PhSUP1*-ox **(D)** plants. Co, cortex; Vb, vascular bundle.

**(E)** and **(F)** Cross-sections of leaves in wild-type **(E)** and *PhSUP1*-ox **(F)** plants. Pl, palisade mesophyll layer; Sp, spongy mesophyll layer.



**Table 1.** Correlation between the Sizes of Organs and Cells

	Length (mm)			Cell Size ( $\mu\text{m}$ )		
	WT	<i>PhSUP1-ox</i>	%WT	WT	<i>PhSUP1-ox</i>	%WT
Peduncle internode	38.6 $\pm$ 3.8	12.7 $\pm$ 1.4	32.9	168.4 $\pm$ 27	66.8 $\pm$ 9.6	39.8
Pedicel	36.9 $\pm$ 2.7	31.2 $\pm$ 2.6	84.6	148.1 $\pm$ 24	121.63 $\pm$ 25	82.1
Petal limb	20.8 $\pm$ 0.9	8.0 $\pm$ 0.4	38.5	20.2	19.6	97.0
Petal tube	52.2 $\pm$ 1.4	38.4 $\pm$ 1.7	73.6	118.2 $\pm$ 23	91.6 $\pm$ 16	77.6

The lengths of peduncle internodes and pedicels are the mean  $\pm$  1 standard deviation of 10 samples, and the cells sizes are the mean  $\pm$  1 standard deviation of 30 cells. The lengths of petal limbs and petal tubes are the mean  $\pm$  1 standard deviation of 15 flowers, and the corresponding cell sizes were estimated from cell numbers in scanning electron micrographs ( $300 \times 258 \mu\text{m}$ ), assuming that cells are approximately round. Cell sizes are in longitudinal direction.

*PhSUP1-ox*, line overexpressing *PhSUP1*.

## DISCUSSION

### *PhSUP1* Is a *P. hybrida* Counterpart of Arabidopsis *SUP*

In this study, we have shown that *PhSUP1* is a *P. hybrida* ortholog of the Arabidopsis *SUP* gene. Introduction of *PhSUP1* genomic DNA into an Arabidopsis *sup* mutant resulted in partial complementation of the early phenotypes (i.e., increased stamen number and defective carpel development) and the late phenotype of loss of bilateral symmetry in ovule development. Transposon-induced mutants displayed *sup*-like phenotypes with respect to stamen number, carpel development, and ovule development. These results indicate that both the early floral meristem function in the floral meristem and the late function in ovule development are common between Arabidopsis *SUP* and *P. hybrida PhSUP1*.

The incompleteness of the complementation may be attributable to differences in protein function or to an imperfect match of the *PhSUP1* promoter activity and the expression pattern of *SUP* in Arabidopsis. Considering the difference in flower structures between the two plant species and the similarity in the phenotypes resulting from overexpression of the two genes (discussed later), the faulty promoter scenario seems the more likely.

Null alleles of Arabidopsis *sup* mutants occasionally exhibited nearly complete loss of carpel formation and increased stamen numbers up to as many as 20. By contrast, *phsup1* mutant *P. hybrida* plants never completely lacked carpels, and the number of extra stamens was at most 3; therefore, the effects of the mutation appear to be less severe in *P. hybrida*. The difference in the number of extra stamens might reflect the size of region of the floral apex, which is predestinate to form whorls 3 and 4, relative to those of stamen primordia. It has been proposed that the number of organs formed in a particular whorl is correlated with the size of each whorl (Meyerowitz, 1997). In Arabidopsis, because the size of floral apex is much larger than that of stamen primordia, more than one ring of extra stamen primordia appear in the floral apex of *sup* mutants. By contrast, the floral apex of *P. hybrida* is only a few times larger than the region occupied by stamen primordia, which might reflect the small number of extra stamens in *phsup1* mutant flowers.

We detected *PhSUP1* transcripts at the bases of developing whorl 2 and whorl 3 organs only after stamen primordia emerged.

This distribution pattern of transcripts is different from the early-stage expression of Arabidopsis *SUP*, which localized in the subdomain of whorl 3 adjacent to whorl 4. Considering that the expression level of *SUP* is low (Sakai et al., 1995), it is possible that we missed very early expression of *PhSUP1* at a stage earlier than that shown in Figure 7A. Therefore, we refrain from discussing early functions of *PhSUP1*, in light of its observed expression, and comparing with those of Arabidopsis *sup*.

### *PhSUP1* Function in Ovule Development

*PhSUP1* plays a role in ovule development of *P. hybrida*, as *SUP* does in Arabidopsis. The conservation of *SUP/PhSUP1* function in ovule development in the two plant species has implications for the evolution of the ovule structure in dicot plants. Whereas the Arabidopsis ovule has two layers of integument (bitegmy), the *P. hybrida* ovule has a single-layer integument (unitegmy). The unitegmic ovule of Asteridae plants, including *P. hybrida*, is thought to have derived from the bitegmic ovules during evolution either by loss of either the outer or inner integument or fusion of the two primordia for outer and inner integuments (Fahn, 1990). Gaiser et al. (1995) found that the role of *SUP* is limited to development of the outer integument. This finding and the fact that *PhSUP1* is involved in the development of the unitegmic ovule in *P. hybrida* argue against the possibility that the *P. hybrida* integument originated from the inner integument.

### *PhSUP1* Function in Intercalary Growth at the Base of Flower Organs

In *P. hybrida*, stamen filaments are fused to the petal tube at their lower portion. This structure results from the intercalary growth of cells between stamen and petal primordia that begins just after emergence of the organ primordia (van der Krol et al., 1993). *phsup1* mutants have some unusual tissues around the bottom of the stamen filaments. These extra tissues appear to connect stamen filaments with petal tubes and also with the ovary, and they seem to have arisen by excessive progression of the intercalary growth in interorgan regions. *PhSUP1* is expressed in the region between organ primordia, which is in agreement with the phenotype observed in this region of *phsup1* mutants. Unlike

in *P. hybrida*, the stamens of Arabidopsis are separated from petals and pistil. In accordance with this difference in flower structure, this extra-tissue phenotype has not been reported for Arabidopsis *sup* mutants. *PhSUP1* may contribute to flower morphogenesis by suppressing over-progression of intercalary growth. Presumably, this particular role of *PhSUP1* has co-evolved with the flower structure of *P. hybrida*.

### **PhSUP1 Function in Placenta Morphogenesis**

*PhSUP1* transcripts were detected around the concave regions at the top and bottom of the placenta in the ovary. In light of this expression pattern, the concavity at the bottom of the placenta appears to be lost in *phsup1* mutants with apparent elongation of the corresponding region, suggesting a role of *PhSUP1* in controlling placenta morphogenesis. This loss-of-concavity phenotype has not been reported for Arabidopsis *sup* mutants. The structure of the ovary is very different between the two plant species: *P. hybrida* forms a placenta on a central axis by axial placentation, whereas in Arabidopsis, placenta originates at the sidewalls of the ovary near the junction of the two carpels. The function of *PhSUP1* in placenta morphogenesis might have co-evolved with the specific type of placentation.

### **PhSUP1 Function in the Morphogenesis of Anther**

Anthers in the *phsup1* mutants showed an aberrant morphology—incomplete development of the interthecal furrow and fusion of inner (adaxial) locules in the upper part. In wild-type anthers, the cells around a vascular bundle are smaller than those in surrounding regions. This control of differential cell growth, which seems to be crucial for normal anther morphogenesis, is lost in *phsup1* mutants (Figure 5). The cells in the connective tissue along the adaxial side appear to be excessively proliferated in *phsup1* mutants. In accordance with these phenotypes, *PhSUP1* transcripts were found in anthers. The *PhSUP1* transcripts are distributed in a band of cells across the interthecal region at the abaxial region of anthers, which is adjacent to the region where cell growth is suppressed in wild-type anthers. *PhSUP1* may function in a non-cell-autonomous manner in anthers, as has been proposed for the early floral meristem function of *SUP* in floral meristems (Sakai et al., 1995). The structures of anthers in *P. hybrida* and Arabidopsis appear quite similar; therefore, it is striking that *PhSUP1* plays a role in anther development in *P. hybrida*, whereas *SUP* does not in Arabidopsis. The function of *SUP* in anther morphogenesis, if any, might be masked by functional redundancy.

Phenotypes similar to those for anther development in *phsup1* mutants have been reported for Arabidopsis *ettin* mutants (Sessions et al., 1997). In anthers, *ETTIN* is expressed in the vascular tissue and in four bands of cells. The adaxial interthecal furrow is poorly developed in *ettin* anthers, causing fusion of two thecae, similar to that seen in *phsup1* mutants. Considering the similarity in the mutant phenotypes, it is of interest whether a gene orthologous to *ETTIN* is involved in anther development in *P. hybrida* and whether there is any functional interaction between *PhSUP1* and the putative *ETTIN* homolog.

### **PhSUP1 Overexpression Phenotypes and Their Implications for PhSUP1 Function**

CaMV 35S promoter-driven ectopic expression of *PhSUP1* resulted in reduced sizes of various organs, although the cellular basis for the size reduction was different for the different organs. Cell numbers were obviously reduced in leaves and petal limbs of *PhSUP1*-ox plants. By contrast, shortening of the inflorescence, especially the peduncles, was primarily because of suppression of cell elongation in the longitudinal direction, whereas the effect on cell number was small. Thus, the phenotypes obtained by ectopic expression suggest that *PhSUP1* functions in the control of both cell division and cell elongation. A role in cell division control is proposed for *SUP* on the basis of its mutant phenotypes (Sakai et al., 1995, 2000). This model perhaps holds true for the early floral meristem function of *PhSUP1*. However, the aberrancy in anther development in *phsup1* mutants suggests a role of *PhSUP1* in the control of cell growth as well because the variation in the size of cells around the vascular bundle in wild-type anthers clearly is lost in *phsup1* mutants. Therefore, this loss-of-function phenotype supports a role of *PhSUP1* in the control of cell growth as well as cell division.

The effects of *SUP* overexpression have been studied using various promoters in both dicot (Kater et al., 2000; Bereterbide et al., 2001; Yun et al., 2002) and monocot (Nandi et al., 2000) plants. Bereterbide et al. (2001) overexpressed *SUP* in *N. tabacum* under the control of the CaMV 35S promoter and observed aberrations in plant architecture and cellular morphology that were mostly similar to those observed in *PhSUP1*-ox *P. hybrida*. However, the reduction in internode cell number observed in the *SUP*-overexpressed (*SUP*-ox) *N. tabacum* was not observed in *PhSUP1*-ox *P. hybrida*. A similar discrepancy is present regarding the effects of *SUP* overexpression on the number and expansion of petal cells. The 35S promoter-driven *SUP* suppresses both cell division and cell elongation in the petals of both *N. tabacum* (Bereterbide et al., 2001) and *P. hybrida* (this article), whereas *Floral Binding Protein1* (*FBP1*) promoter-driven *SUP* in *P. hybrida* petals affected cell elongation but not cell number (Kater et al., 2000). Bereterbide et al. speculated that the discrepancy between the phenotypes may be because of a difference in strength of the two promoters in these plants. A similar situation may account for the difference in the internode phenotypes between the *PhSUP1*-ox *P. hybrida* and *SUP*-ox *N. tabacum*. Although the CaMV 35S promoter was used for both transformants, the strength of this promoter is known to differ between these two plant species and may have led to the different phenotypes even when the *SUP* and *PhSUP1* proteins are functionally equivalent. Furthermore, the timing of promoter activation may be a crucial factor that accounts for the different phenotypes resulting from 35S versus *FBP1* promoter-driven *SUP*. Cell elongation in petals and stamens mainly occurs after cell division has completed. If the *FBP1* promoter becomes active later during flower development than does the 35S promoter, the different effects of *SUP* overexpression between the two transformants may be ascribed to that difference in timing. On the basis of these considerations, taken together with the *phsup1* mutant phenotype in anther that is related to cell growth, it seems reasonable to consider that *SUP/PhSUP1* is involved in

the control of both division and growth of cells. Recent studies by Yun et al. (2002) in *Arabidopsis* suggest that, in addition to indirect effects via cell proliferation control, *SUP* has a direct suppressive effect on the expression of class B homeotic genes on the basis of the observation that *SUP* overexpression driven by the *AP1* promoter caused homeotic conversion of petals to stamen. Such homeotic effect was not observed in our *PhSUP1* overexpression experiment in the *P. hybrida* system. The *AP1* promoter is active before homeotic genes are active, whereas the 35S promoter may not be strong enough to cause the homeotic effects in early floral meristems in *P. hybrida*. Therefore, our results do not exclude the possibility that *PhSUP1* has a direct effect on the expression of class B genes.

In summary, we have shown that the *SUP* gene and its early floral meristem function and late function in ovule development, originally discovered in *Arabidopsis*, are conserved in another dicot plant, *P. hybrida*, indicating the generality of this gene function. Furthermore, we have shown that *PhSUP1* has some additional functions unique for *P. hybrida*. These specific functions have implications regarding the roles of *PhSUP1* in the diversification in flower structure. Further comparative studies of *SUP* orthologous genes in various plant species likely will provide further insight into the roles of this important gene in the floral structure specification.

## METHODS

### Isolation of the *PhSUP1* Gene

Nested PCR was performed to amplify partial sequences of *SUP*-like zinc-finger genes using *P. hybrida* (cv Mitchell diploid) genomic DNA as a template. The QALGGH primer [5'-CA(A/G)GCI (T/C)TIGGIGGICA-(C/T)-3'], corresponding to a conserved sequence in zinc-finger domain, and the LDLELR primer [5'-A(G/A)C(T/G)IA(G/A)(T/C)TCIA(G/A)(G/A)-TC-3'], corresponding to a conserved sequence in the C-terminal region, were used for the first round of PCR, and the LGGHMN primer [5'-(T/C)TIGGIGGICA(C/T)ATGAA(C/T)-3'] and the LDLELR primer for the second round. The PCR products were separated by agarose gel electrophoresis, cloned into the pCR II vector (Invitrogen, San Diego, CA), and sequenced. A *PhSUP1* cDNA clone (pSP-*cPhSUP1*) was isolated from a *P. hybrida* ovary cDNA library, which had been constructed in the pSPORT1 vector (Life Technologies, Rockville, MD), using the Gene Trapper positive selection system (Life Technologies) according to the manufacturer's instructions. A genomic DNA library of *P. hybrida* (cv Mitchell diploid) was constructed in the  $\lambda$ EMBL3 vector. A *PhSUP1* genomic clone ( $\lambda$ *gPhSUP1*) was isolated from the genomic DNA library by plaque hybridization screening using the *PhSUP1* cDNA as a probe. A 3.8-kb DNA fragment containing 5'-upstream (2.5 kb), coding, and 3'-UTR (0.46 kb) regions of *PhSUP1* was excised from the  $\lambda$ *gPhSUP1* DNA using *Sall* and *EcoRI* and cloned into pBluescript SK+ (pBS SK+; Stratagene, La Jolla, CA) cleaved with the same set of restriction enzymes, yielding the subclone pBS-*gPhSUP1S-E*.

### Vector Construction

#### *PhSUP1*:*GUS*

An *XbaI-EcoRI* fragment containing the *GUS* coding sequence and *Nos* terminator was excised from pBI121 (Clontech, Palo Alto, CA) and inserted into pUCAP (pUC-*GUS*:*Tnos*). The upstream region of *PhSUP1*

(2.5 kb) was amplified by PCR with the M13 forward (Stratagene) and *PhSUP1*-ATG-*Bam* primers (5'-ATTGGATCCCTCCATGCCTGCC-TAC-3') using pBS-*gPhSUP1S-E* as a template. The *PhSUP1*-ATG-*Bam* primer was designed to introduce a *Bam*HI site just downstream of the *PhSUP1* initiation codon. The PCR fragment was digested with *Sall* and *Bam*HI and cloned into pBS SK+ (pBS-*PhSUP1-Bm*). The cloned fragment was partially sequenced from the 3'-end to confirm the absence of any mutation within 500 bp upstream of the *PhSUP1* initiation codon. A *Sall-Bst*XI fragment (from -2.5 kb to -360 bp upstream of *PhSUP1* initiation codon) of pBS-*PhSUP1-Bm* was replaced with a corresponding sequence excised from pBS-*gPhSUP1S-E* to obtain pBS-*PhSUP1*:*Bm*, which contained the 2.5-kb *PhSUP1* upstream region with a *Bam*HI site at its 3'-end. The *PhSUP1* upstream fragment was excised from pBS-*PhSUP1*:*Bm* using *Pst*I and *Bam*HI and inserted into pUC-*GUS*:*Tnos* upstream of the *GUS* coding sequence using the same sets of restriction enzymes (pUC-*PhSUP1*:*GUS*:*Tnos*). Subsequently, the *PhSUP1*:*GUS*:*Tnos* chimeric gene was excised from pUC-*PhSUP1*:*GUS*:*Tnos* by *Pac*I and *Asc*I and cloned into pBINPLUS using the same sets of restriction enzymes, thereby producing pBIN-*PhSUP1*:*GUS*:*Tnos*.

#### *gPhSUP1*

For the complementation test of the *Arabidopsis sup* mutant by *PhSUP1*, pBIN-*gPhSUP1*:*Tnos*, a derivative of pBINPLUS that contained the *PhSUP1* genomic sequence, was constructed as follows. A 3.8-kb *Sall-Bam*HI fragment containing the upstream (2.5 kb), coding, and 3'-UTR (0.46 kb) sequences of *PhSUP1* was excised from pBS-*gPhSUP1S-E* and placed upstream of the *nos* terminator in pUCAP-*nos*, in which the *nos* terminator had been inserted into the *Sac*I-*Eco*RI site of pUCAP (van Engelen et al., 1995), yielding pUC-*gPhSUP1*SB:*Tnos*. Because pUC-*gPhSUP1*SB:*Tnos* lacked part of the 3'-UTR of *PhSUP1*, the 3'-UTR was recruited from *PhSUP1* cDNA (pSP-*cPhSUP1*) to form pUC-*gPhSUP1*:*Tnos*. Then, the *gPhSUP1*:*Tnos* fragment was shuttled from pUC-*gPhSUP1*:*Tnos* to pBINPLUS (van Engelen et al., 1995) to generate pBIN-*gPhSUP1*:*Tnos*.

#### *P*<sub>35S</sub>:*PhSUP1*

Into the pUCAP plasmid (van Engelen et al., 1995), the CaMV 35S promoter was inserted between the *Hind*III and *Bam*HI sites, and *nopaline synthase* terminator (*Tnos*) sequences were inserted between the *Sac*I and *Eco*RI sites to generate pUC-*P*<sub>35S</sub>:*Tnos*. A *Sall-Not*I fragment containing a complete *PhSUP1* cDNA sequence was excised from pSP-*cPhSUP1* and inserted into pUC-*P*<sub>35S</sub>:*Tnos* between the 35S promoter and the *nos* terminator (pUC-*P*<sub>35S</sub>:*PhSUP*:*Tnos*). A fragment containing the *P*<sub>35S</sub>:*PhSUP1*-*Tnos* chimeric gene was excised from pUC-*P*<sub>35S</sub>:*PhSUP1*:*Tnos* using *Asc*I and *Pac*I and was introduced into the binary vector pBINPLUS (van Engelen et al., 1995) to yield pBIN-*P*<sub>35S</sub>:*PhSUP1*:*Tnos*.

### Plant Materials and Transformation

Mutant alleles for *PhSUP1* were isolated by screening libraries of *dTph1*-inserted mutant lines using a PCR-based method (Koes et al., 1995). A primer complementary to a terminal repeat of *dTph1* (*Out-1*) and one of two *PhSUP1*-specific primers (*PhSUP1*-UPS, 5'-ATTCTGCTAGTT-GTCCCCTTGAT-3', and *PhSUP1*-DS, 5'-ATTTTTGCATCTTCACTCCTG-3') were used for each amplification. *PhSUP1* sequences in *dTph1*-inserted alleles were amplified by PCR with the *PhSUP1*-UPS and *PhSUP1*-DS primers, cloned into the pCR II vector (Invitrogen), and sequenced. Transformation of *P. hybrida* cv Mitchell diploid was performed by the *A. tumefaciens*-mediated method (Jorgensen et al., 1996).



All *Arabidopsis* plants that were used in this study were of the Columbia (Col-0) ecotype. The *sup* mutant used in this study carried the *sup-2* (*flo10*, Schultz et al., 1991) allele and was obtained from the ABRC seed stock center. Complementation of the *sup* mutant by the *PhSUP1* genomic DNA fragment was performed as follows. The binary vector pBIN-*gPhSUP1*-NT, which contains the upstream and coding sequences of *PhSUP1*, was introduced into *A. tumefaciens* strain GV3101. This bacterial strain was used to transform wild-type *Arabidopsis* plants by the vacuum infiltration method (Bechtold and Pelletier, 1998). Kanamycin-resistant transformants were crossed with the *sup-2* mutant, and resulting F1 plants were self-pollinated. From among the F2 plants, homozygous *sup-2* mutant plants harboring a *PhSUP1* transgene were selected and characterized. The presence of the *PhSUP1* transgene in each F2 plant was confirmed by PCR amplification of the *PhSUP1* sequence using the PhSUP1-UPS and PhSUP1-DS primers. The genotype of the *SUP* locus in each F2 plant was analyzed by examining the *NcoI* restriction pattern of the *SUP* locus after PCR amplification with *SUP*-specific primers (AtSUP-U1, 5'-GCATAGCCAAAAGAAAGAGC-3', and AtSUP-D2, 5'-GGGTAAGGAGGAGAAGGTGTT-3'). *NosI* cleaves the wild-type *SUP* sequence but not that of the *sup-2* allele.

### Microscopy

For light microscopy, *P. hybrida* tissues were fixed in FAA (formalin:acetic acid:ethanol:water, 10:5:50:35), dehydrated in an ethanol series, embedded in Historesin (Leica Microsystems, Wetzlar, Germany), and sectioned at 2 to 4  $\mu\text{m}$ . The sections were stained in a 1% solution of toluidine blue. For interference contrast microscopy, tissues were fixed in fixation solution (ethanol:acetic acid, 90:10) and cleared by chloral hydrate treatment. For scanning electron microscopy, tissues were frozen in liquid nitrogen and observed through a Hitachi S-2380 (Hitachi Science Systems, Hitachinaka, Japan) under low vacuum.

### In Situ Hybridization

Tissues were fixed in FAA at 4°C for 48 h, dehydrated in an ethanol series and then a tertiary butanol series, and embedded in Paraplast Plus (Sigma, St. Louis, MO). The paraffin-embedded tissues were sectioned to 5- $\mu\text{m}$  thickness, affixed on microscopic slides by incubating at 42°C overnight, and used for in situ hybridization. Template plasmids for probe RNA synthesis were constructed as follows. With the *PhSUP1* cDNA (pSP-*cPhSUP1*) as a template, a 750-bp PCR fragment beginning downstream of the zinc-finger region of *PhSUP1* was amplified using the T7-SPL1-2 primer (5'-TAATACGACTCACTATAGGGAGAGGCTTAGAC-TACAATCAC-3', with the T7 promoter sequence underlined) and the T3-SPL1-3RV primer (5'-AATTAACCCTCACTAAAGGGCATCTAGAGAA-GATAGT-3', with the T3 promoter sequence underlined) so that sense and antisense *PhSUP1*-specific RNA probes could be transcribed from each end. With the PCR fragment as a template, digoxigenin (DIG)-labeled RNA probes were synthesized using a DIG RNA labeling kit (Roche Diagnostics, Basel, Switzerland). In situ hybridization procedures, from pretreatment to staining, were performed using an automatic staining module, the Discovery HX system (Ventana Medical Systems, Tucson, AZ). Pretreatment, hybridization, and washing of sections were performed using the RiboMapKit (Ventana Medical Systems) according to the manufacturer's instructions. Sections were hybridized with DIG-labeled probes in RiboHybe (Ventana) hybridization solution at 67°C for 6 h. After hybridization, the sections were washed three times in 0.1 $\times$  SSC (1 $\times$  SSC is 0.15 M NaCl and 0.015 M sodium citrate) (70°C, 6 min). Hybridization signals were then detected with horseradish peroxidase-conjugated antidigoxigenin antibody (Roche Diagnostics), enhanced with an AmpMapKit (Ventana), which is based on the tyramide signal amplification reaction, and developed using the BlueMapKit (Ventana).

The stained slides were dehydrated through an ethanol series, washed twice in xylene, and mounted in MX mounting medium (Matsunami Glass, Osaka, Japan).

### RNA Gel Blot Hybridization

Total RNA was isolated from tissues homogenized in liquid nitrogen using the RNeasy plant kit (Qiagen, Hilden, Germany). Aliquots (10  $\mu\text{g}$ ) of total RNA were separated on a 1.2% agarose gel containing 0.4 M formaldehyde and blotted onto GeneScreen membranes (NEN Life Science Products, Boston, MA). Antisense DIG-labeled probe was synthesized as described for the in situ hybridization procedure. The blotted membranes were hybridized with the DIG-labeled probe, and signals were detected by a chemiluminescence reaction using a DIG nucleic acid detection kit (Roche Diagnostics) and CDP-STAR (Roche Diagnostics). The chemiluminescence signals were detected by exposing the treated membranes to Lumi-films (Roche Diagnostics).

### RT-PCR

Poly(A)<sup>+</sup> RNA was purified from total RNA using the QuickPrep Micro mRNA purification kit (Amersham Pharmacia Biotech, Buckinghamshire, UK) and was treated with DNase I. First-strand cDNA was synthesized from an aliquot of DNase poly(A)<sup>+</sup> RNA using the Superscript pre-amplification system (Gibco BRL, Cleveland, OH). An aliquot of first-strand cDNA was subjected to 30 cycles of PCR amplification with *PhSUP1*-specific primers (SPL1U2-23, 5'-GGCAGGCATGGAGAAAA-CAATA-3', and SPL1D2-24, 5'-TTCAGACCTCTTCATCAACACTTC-3'). A negative-control reaction lacking reverse transcriptase was performed to assess contamination with genomic DNA. The amount of template cDNA was normalized by PCR with a ubiquitin-specific primer pair (PetUBQ1-5', 5'-GCCACTCTTCTCCTTCTATTC-3', and PetUBQ1-3', 5'-CTTCTTCTACGCTTCTTGC-3').

Sequence data from this article have been deposited with the EMBL/GenBank data libraries under accession number AB117749.

### ACKNOWLEDGMENTS

We thank Hiroshi Kouchi for providing unpublished sequence information of a *G. max* zinc-finger gene. This work was supported by a Center of Excellence Promotion Fund from the Science and Technology Agency of Japan and by a PROBRAIN grant from the Bio-Oriented Technology Research Advancement Institution of Japan.

Received October 30, 2003; accepted January 24, 2004.

### REFERENCES

- Angenent, G.C., Franken, J., Busscher, M., Colombo, L., and van Tunen, A.J. (1993). Petal and stamen formation in petunia is regulated by the homeotic gene *fbp1*. *Plant J.* **4**, 101–112.
- Bechtold, N., and Pelletier, G. (1998). In planta *Agrobacterium*-mediated transformation of adult *Arabidopsis thaliana* plants by vacuum infiltration. *Methods Mol. Biol.* **82**, 259–266.
- Bereterbide, A., Hernould, M., Castera, S., and Mouras, A. (2001). Inhibition of cell proliferation, cell expansion and differentiation by the *Arabidopsis SUPERMAN* gene in transgenic tobacco plants. *Planta* **214**, 22–29.

- Bowman, J.L., Sakai, H., Jack, T., Weigel, D., Mayer, U., and Meyerowitz, E.M.** (1992). *SUPERMAN*, a regulator of floral homeotic genes in *Arabidopsis*. *Development* **114**, 599–615.
- Clark, S.E., Running, M.P., and Meyerowitz, E.M.** (1993). *CLAVATA1*, a regulator of meristem and flower development in *Arabidopsis*. *Development* **119**, 397–418.
- Colombo, L., Franken, J., Koetje, E., van Went, J., Dons, H.J., Angenent, G.C., and van Tunen, A.J.** (1995). The petunia MADS box gene *FBP11* determines ovule identity. *Plant Cell* **7**, 1859–1868.
- Dathan, N., Zaccaro, L., Esposito, S., Isernia, C., Omichinski, J.G., Riccio, A., Pedone, C., Di Blasio, B., Fattorusso, R., and Pedone, P.V.** (2002). The *Arabidopsis* *SUPERMAN* protein is able to specifically bind DNA through its single Cys2-His2 zinc finger motif. *Nucleic Acids Res.* **30**, 4945–4951.
- Fahn, A.** (1990). Reproductive organs. In *Plant Anatomy*, A. Fahn, ed (Oxford, UK: Pergamon Press), pp. 411–488.
- Ferrario, S., Immink, R.G., Shchennikova, A., Busscher-Lange, J., and Angenent, G.C.** (2003). The MADS box gene *FBP2* is required for *SEPALLATA* function in petunia. *Plant Cell* **15**, 914–925.
- Gaiser, J.C., Robinson-Beers, K., and Gasser, C.S.** (1995). The *Arabidopsis* *SUPERMAN* gene mediates asymmetric growth of the outer integument of ovules. *Plant Cell* **7**, 333–345.
- Goto, K., and Meyerowitz, E.M.** (1994). Function and regulation of the *Arabidopsis* floral homeotic gene *PISTILLATA*. *Genes Dev.* **8**, 1548–1560.
- Hiratsu, K., Ohta, M., Matsui, K., and Ohme-Takagi, M.** (2002). The *SUPERMAN* protein is an active repressor whose carboxy-terminal repression domain is required for the development of normal flowers. *FEBS Lett.* **514**, 351–354.
- Ito, T., Sakai, H., and Meyerowitz, E.M.** (2003). Whorl-specific expression of the *SUPERMAN* gene of *Arabidopsis* is mediated by cis elements in the transcribed region. *Curr. Biol.* **13**, 1524–1530.
- Jack, T., Brockman, L.L., and Meyerowitz, E.M.** (1992). The homeotic gene *APETALA3* of *Arabidopsis thaliana* encodes a MADS box and is expressed in petals and stamens. *Cell* **68**, 683–697.
- Jorgensen, R.A., Cluster, P.D., English, J., Que, Q., and Napoli, C.A.** (1996). *Chalcone synthase* cosuppression phenotypes in petunia flowers: Comparison of sense vs. antisense constructs and single-copy vs. complex T-DNA sequences. *Plant Mol. Biol.* **31**, 957–973.
- Kapoor, M., Tsuda, S., Tanaka, Y., Mayama, T., Okuyama, Y., Tsuchimoto, S., and Takatsui, H.** (2002). Role of petunia *pMADS3* in determination of floral organ and meristem identity, as revealed by its loss of function. *Plant J.* **32**, 115–127.
- Kater, M.M., Franken, J., van Aelst, A., and Angenent, G.C.** (2000). Suppression of cell expansion by ectopic expression of the *Arabidopsis* *SUPERMAN* gene in transgenic petunia and tobacco. *Plant J.* **23**, 407–413.
- Koes, R., et al.** (1995). Targeted gene inactivation in petunia by PCR-based selection of transposon insertion mutants. *Proc. Natl. Acad. Sci. USA* **92**, 8149–8153.
- Krizek, B.A., and Meyerowitz, E.M.** (1996). The *Arabidopsis* homeotic genes *APETALA3* and *PISTILLATA* are sufficient to provide the B class organ identity function. *Development* **122**, 11–22.
- Meyerowitz, E.M.** (1997). Genetic control of cell division patterns in developing plants. *Cell* **88**, 299–308.
- Nandi, A.K., Kushalappa, K., Prasad, K., and Vijayraghavan, U.** (2000). A conserved function for *Arabidopsis* *SUPERMAN* in regulating floral-whorl cell proliferation in rice, a monocotyledonous plant. *Curr. Biol.* **10**, 215–218.
- Sakai, H., Krizek, B.A., Jacobsen, S.E., and Meyerowitz, E.M.** (2000). Regulation of *SUP* expression identifies multiple regulators involved in *Arabidopsis* floral meristem development. *Plant Cell* **12**, 1607–1618.
- Sakai, H., Medrano, L.J., and Meyerowitz, E.M.** (1995). Role of *SUPERMAN* in maintaining *Arabidopsis* floral whorl boundaries. *Nature* **378**, 199–203.
- Schultz, E.A., Pickett, F.B., and Haughn, G.W.** (1991). The *FLO10* gene product regulates the expression domain of homeotic genes *AP3* and *PI* in *Arabidopsis* flowers. *Plant Cell* **3**, 1221–1237.
- Sessions, A., Nemhauser, J.L., McColl, A., Roe, J.L., Feldmann, K.A., and Zambryski, P.C.** (1997). *ETTIN* patterns the *Arabidopsis* floral meristem and reproductive organs. *Development* **124**, 4481–4491.
- Smyth, D.R., Bowman, J.L., and Meyerowitz, E.M.** (1990). Early flower development in *Arabidopsis*. *Plant Cell* **2**, 755–767.
- Tsuchimoto, S., van der Krol, A.R., and Chua, N.-H.** (1993). Ectopic expression of *pMADS3* in transgenic petunia phenocopies the petunia *blind* mutant. *Plant Cell* **5**, 843–853.
- van der Krol, A.R., Brunelle, A., Tsuchimoto, S., and Chua, N.-H.** (1993). Functional analysis of petunia floral homeotic MADS box gene *pMADS1*. *Genes Dev.* **7**, 1214–1228.
- van der Krol, A.R., and Chua, N.-H.** (1991). The basic domain of plant B-ZIP proteins facilitates import of a reporter protein into plant nuclei. *Plant Cell* **3**, 667–675.
- van Engelen, F.A., Molthoff, J.W., Conner, A.J., Nap, J.P., Pereira, A., and Stiekema, W.J.** (1995). *pBINPLUS*: An improved plant transformation vector based on *pBIN19*. *Transgenic Res.* **4**, 288–290.
- Yanofsky, M.F., Ma, H., Bowman, J.L., Drews, G.N., Feldmann, K.A., and Meyerowitz, E.M.** (1990). The protein encoded by the *Arabidopsis* homeotic gene *AGAMOUS* resembles transcription factors. *Nature* **346**, 35–39.
- Yun, J.Y., Weigel, D., and Lee, I.** (2002). Ectopic expression of *SUPERMAN* suppresses development of petals and stamens. *Plant Cell Physiol.* **43**, 52–57.